Available online at www.sciencedirect.com
SCIENCE DIRECT
International Journal of Mass Spectrometry 248 (2006) 142–147
International Journal of Mass Spectrometry
www.elsevier.com/locate/ijms

An analysis of the evolution of negative ions produced by a corona ionizer in air

Kenkichi Nagato [a,*], Yasunori Matsui [b], Takahiro Miyata [b], Toshiyuki Yamauchi [b]

[a] *Kochi National College of Technology, Nankoku 783-8508, Japan*
[b] *Home Appliance R&D Laboratory, Matsushita Electric Works Ltd., Kadoma 571-8686, Japan*

Received 13 October 2005; received in revised form 3 December 2005; accepted 5 December 2005
Available online 18 January 2006

Abstract

Mass spectrometric measurements of negative ions produced by a dc corona ionizer in air were conducted at different reaction times (ca. 1.0 ms and 10 ms) to observe the evolution of negative ions in air. One of the characteristic features was the rapid dominance of NO_3^- ions in the mass spectra, which is indicative of the strong influence of O_3 and NO_2 produced by discharge in the early stages of negative ion evolution. Water vapor was also found to play a significant role in NO_3^- ion formation. The production of OH radicals by ion–molecule reactions involving H_2O leads to the formation of HNO_3 which accelerates the conversion of primary negative ions to NO_3^- ions. As a result, NO_3^- and $NO_3^-HNO_3$ ions were observed as terminal ions. Another terminal ion observed was assigned to $HCO_3^-HNO_3$. The reaction of OH^- with CO_2 is probably responsible for the formation of HCO_3^-. From considerations of ion reactivity, NO_3^- ions likely represent the most long-lived ion species in negative ion evolution in indoor air.

Keywords: Corona discharge; Negative air ion; Ion evolution; Ion–molecule reaction; Mass spectrometry

1. Introduction

Corona discharge ionizers are widely used to generate ions in air. They are typically installed in commercial electrical appliances such as air cleaners and air conditioners because negative ions have been reported to reduce the levels of particulates, airborne microbes, odors and volatile organic compounds in indoor air [1,2]. However, the detailed mechanisms by which negative air ions contribute to improving indoor air quality are not clearly understood.

Information on the ion composition produced by such devices is essential if we are to understand the role of ions in air cleaning processes. Mass spectrometry has been used to identify ions produced by corona sources [3–9]. A variety of negative ion species have been identified. Included among these are O^-, O_2^-, O_3^-, CO_3^-, CO_4^-, HCO_3^-, NO_2^- and NO_3^- ions. The relative abundance of the detected ions appears to vary depending on the condition of the air used in the measurements.

Not all of the above ions persist for very long in air. Due to successive ion–molecule reactions, they evolve to form more stable ions. Therefore, identifying ions that have long lifetimes in air is an important issue in the study of the role of such ions in indoor air cleaning. Few mass spectrometric studies have been reported on ion evolution in air, but a number of modeling efforts have been carried out. The evolution of negative ions in the tropospheric atmosphere has been simulated by Huertas et al. [10]. Their results indicated that the terminal ions formed in a time shorter than 10^{-5} s were $O_2^-(H_2O)_n$ and lesser amounts of $CO_4^-(H_2O)_n$, $CO_3^-(H_2O)_n$ and $HCO_3^-(H_2O)_n$ were formed. Luts [11] calculated negative ion evolution up to 100 s and showed that minor constituents such as HNO_3 and H_2SO_4 participate in the reactions after 0.1 s to form NO_3^- and HSO_4^- ions. However, these calculations were carried out for normal air conditions. In cases of discharges in air, not only ions but O_3, NO_x, and radicals are also known to be produced. These byproducts significantly influence ion–molecule reactions occurring near the discharge area [7], hence the lifetimes of individual ions may be modified.

The aim of this study was to observe the evolution of negative ions produced by a negative corona ionizer and to determine

* Corresponding author. Tel.: +81 88 864 5641; fax: +81 88 864 5641.
E-mail address: nagato@me.kochi-ct.ac.jp (K. Nagato).

1387-3806/$ – see front matter © 2005 Elsevier B.V. All rights reserved.
doi:10.1016/j.ijms.2005.12.001

the ion species which persist for relatively long periods in air. Obviously observing the entire ion evolution is difficult because the lifetime of an ion in indoor air can be as long as 10^2 s. In the present study, we focused on observing changes in negative ion species around a few milliseconds after ionization, at which times the formation of stable negative ions would be expected to start.

2. Experimental apparatus

The ion mobility spectrometer/mass spectrometer (IMS/MS) employed in measurements is schematically shown in Fig. 1. The details of the instrument have been described previously [12]. The drift tube is constructed of stainless steel guard rings (58 mm i.d.) separated by Macor spacers. It is sealed using O-rings and is operated at atmospheric pressure. The guard rings are connected by a series of 1 MΩ resistors. By applying a high voltage between both ends of the resistor chain, a uniform electric field is produced in the drift tube.

A corona ionizer, consisting of a discharge needle and a ring electrode (12 mm i.d.) was adapted for use in this study. The needle and the ring electrode were made of stainless steel, and the distance between the needle tip and the center of the ring was 3 mm. A discharge voltage of −4.5 kV was applied to the needle relative to the ring electrode. With this setting, the discharge current was 8.5–10.5 μA in both ambient and purified air. Ions which enter the drift tube travel along the electric field and can react with surrounding neutral molecules until they arrive at the orifice plate. Thus, the reaction time of ions depends on the length of the drift region, the intensity of the electric field, and the mobilities of the ions.

In order to observe ion evolution, mass spectrometric measurements were made using two different drift tube configurations: one was with no guard rings and the other with three guard rings. In the case where no guard rings were used, the ring electrode was placed 19.5 mm in front of the orifice plate. A voltage of −2 kV was applied to the ring electrode relative to the grounded orifice plate. Assuming that the mobility of the negative ions was 2.0 $cm^2\ V^{-1}\ s^{-1}$, the estimated reaction time for them was 1.0 ms. In the case of three guard rings, the potential difference across the drift tube was −1.5 kV and an additional voltage of −0.5 kV was applied to the ring electrode relative to the guard ring nearest the ring electrode. The distance between the ring electrode and the orifice plate was 64.5 mm and the ion reaction time was approximately 10 ms.

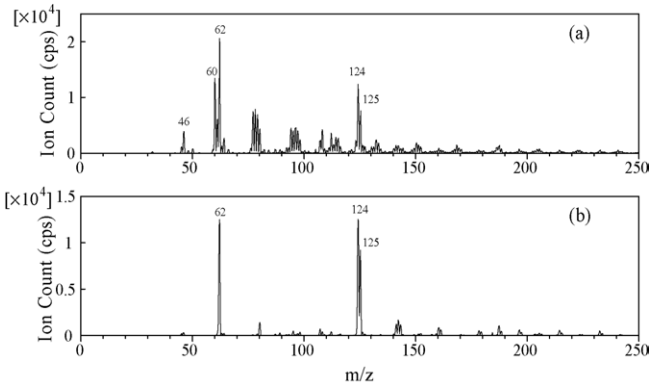

Fig. 2. Negative ion mass spectra in ambient air for two different reaction times: (a) 1.0 ms; (b) 10 ms.

3. Results and discussion

3.1. Mass spectra of negative ions in ambient air

Fig. 2 shows mass spectra of negative ions in ambient air. The temperature and the relative humidity were 24 °C and 30%, respectively. The spectrum obtained with no guard rings is shown in Fig. 2(a). A number of ion peaks were observed in the spectrum, indicating that many competing reactions were taking place in the early stage of the negative ion evolution. Table 1 summarizes the assignments for the major ions. The remainder of the ion peaks in the spectrum corresponded to hydrated ions

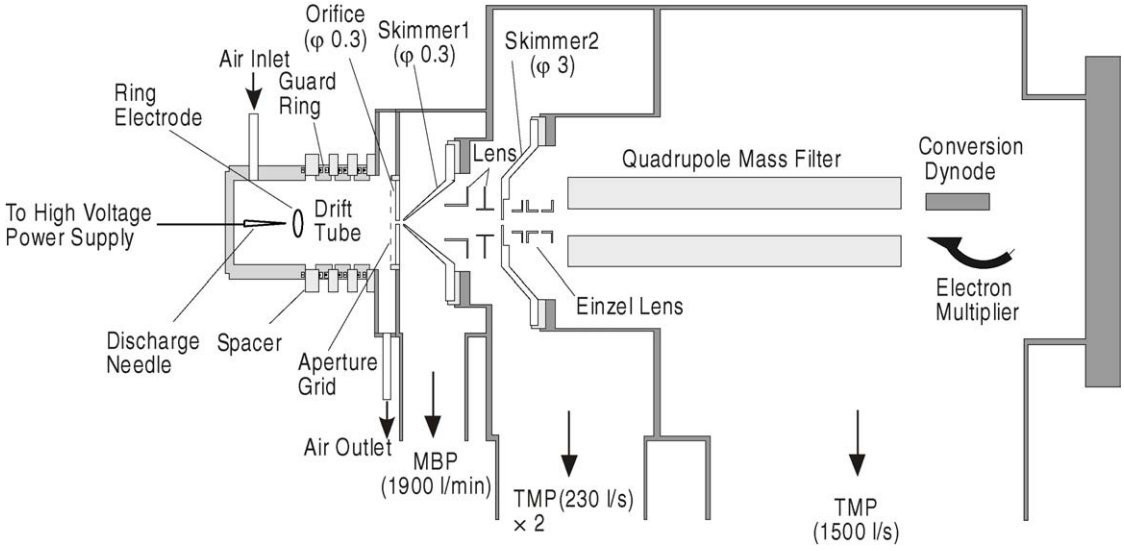

Fig. 1. Schematic representation of the IMS/MS.

Table 1
Summary of peak assignments in the mass spectrum shown in Fig. 2(a)

m/z	Assignment
32	O_2^-
46	NO_2^-
48	O_3^-
60	CO_3^-
61	HCO_3^-
62	NO_3^-
76	CO_4^-
77	HCO_4^-
108	$NO_3^-NO_2$
109	$NO_2^-HNO_3$
123	$CO_3^-HNO_3$
124	$HCO_3^-HNO_3$
125	$NO_3^-HNO_3$

of the ions listed in Table 1. Among the detected ions, CO_3^- ($m/z = 60$), NO_3^- (62), $HCO_3^-HNO_3$ (124), and $NO_3^-HNO_3$ (125) were abundant ion species.

Fig. 2(b) shows the mass spectrum obtained using three guard rings. A marked decrease in ion signals other than those of NO_3^-, $HCO_3^-HNO_3$, and $NO_3^-HNO_3$ was observed.

The identifications of the key ions and the relevant reactions are discussed in the following sections.

3.2. Formation of NO_3^- ions

The dominance of NO_3^- core ions is a characteristic feature of a negative corona discharge in air as can be seen in Fig. 2. This can be attributed to the production of O_3 and NO_2 by discharge in air. The O_3 and NO_2 concentrations were monitored using an ozone monitor and a NO_x monitor. Under the present experimental conditions using ambient air, the concentrations of O_3 and NO_2 were about 1 ppm and 0.1–0.2 ppm, respectively, greater than in normal air. The enhancement of both O_3 and NO_2 can promote the efficient formation of NO_3^- via several pathways as follows [5,13,14].

The primary negative ions generated in a corona discharge are O^- and O_2^-. Both react with NO_2 to form NO_2^-, which can be converted to NO_3^- by a reaction with O_3 [15]:

$$O^- + NO_2 \rightarrow NO_2^- + O, \qquad k_1 = 1.0 \times 10^{-9}\,cm^3/s \quad (1)$$

$$O_2^- + NO_2 \rightarrow NO_2^- + O_2, \qquad k_2 = 7 \times 10^{-10}\,cm^3/s \quad (2)$$

$$NO_2^- + O_3 \rightarrow NO_3^- + O_2, \qquad k_3 = 1.2 \times 10^{-10}\,cm^3/s \quad (3)$$

The O^- and O_2^- ions also react with O_3 to produce O_3^-. NO_3^- ions are then formed by the reaction with O_3^- and NO_2 [15]:

$$O^- + O_3 \rightarrow O_3^- + O, \qquad k_4 = 8.0 \times 10^{-10}\,cm^3/s \quad (4)$$

$$O_2^- + O_3 \rightarrow O_3^- + O_2, \qquad k_5 = 6 \times 10^{-10}\,cm^3/s \quad (5)$$

$$O_3^- + NO_2 \rightarrow NO_3^- + O_2, \qquad k_6 = 2.8 \times 10^{-10}\,cm^3/s \quad (6)$$

The reactions of CO_2 with O^- and O_3^- lead to the formation of CO_3^- ions, which subsequently reacts with NO_2 to form NO_3^- [15,16]:

$$O^- + CO_2 + M \rightarrow CO_3^- + M, \qquad k_7 = 3.1 \times 10^{-28}\,cm^6/s \quad (7)$$

$$O_3^- + CO_2 \rightarrow CO_3^- + O_2, \qquad k_8 = 5.5 \times 10^{-10}\,cm^3/s \quad (8)$$

$$CO_3^- + NO_2 \rightarrow NO_3^- + CO_2, \qquad k_9 = 2 \times 10^{-10}\,cm^3/s \quad (9)$$

Ross and Bell [7], by employing a reverse flow continuous discharge ionization technique, confirmed that neutral species that are formed in a corona discharge strongly influence the formation of O_3^-, CO_3^-, and NO_3^- ions.

In some of the previous studies [4,9], CO_3^- ions were predominantly observed in the mass spectra of negative ions produced by a negative corona discharge in air. This difference in dominant ion species between the present result and previous studies may be due to different reaction times of the ions. In the experiments reported by Gardiner and Craggs [4] and Skalny et al. [9], negative ions were produced under relatively low pressure conditions and were immediately sampled through a pin hole in the anode. In the measurements reported here, ions were produced at atmospheric pressure and then moved through the drift tube for at least 1 ms until reaching the sampling orifice. Since the dominant reaction of CO_3^- ions in air is reaction (9) [5,14], the production of NO_3^- ions would proceed as the reaction time increased. The characteristic time for this conversion under the present experimental condition is estimated to be 1.2 ms using the reaction rate constant ($2 \times 10^{-10}\,cm^3/s$) and a NO_2 concentration of 0.15 ppm. The results of this calculation are in agreement with the disappearance of CO_3^- ions in the mass spectrum shown in Fig. 2(b) (ion reaction time: 10 ms) while they were present in the spectrum shown in Fig. 2(a) (1.0 ms).

3.3. Formation of HNO_3

The results of this study confirm the formation of HNO_3 in a corona discharge in air, since ions associated with HNO_3: $CO_3^-HNO_3$, $HCO_3^-HNO_3$, and $NO_3^-HNO_3$ were detected. Since the electron affinity of HNO_3 is large among neutral species in air, HNO_3 reacts with most of the primary negative ions to form NO_3^- ions [17]. Therefore, HNO_3 formed by the discharge plays an important role in negative ion evolution: negative ions are efficiently converted to NO_3^- by reactions with HNO_3. This could be another reason for why negative ions other than NO_3^- ions declined rapidly as shown in Fig. 2(b).

We conclude that the production of HNO_3 is strongly dependent on the concentration of H_2O. Fig. 3 shows the negative ion mass spectra at three different H_2O concentrations in purified air. The measurements were made with three guard rings (reaction time: 10 ms). In dry air (H_2O: 25 ppm), NO_3^- predominated and the abundance of $NO_3^-HNO_3$ ion was very small, indicating that HNO_3 formation was not very prominent. However, as the H_2O concentration increased, the abundance of the $NO_3^-HNO_3$ ion

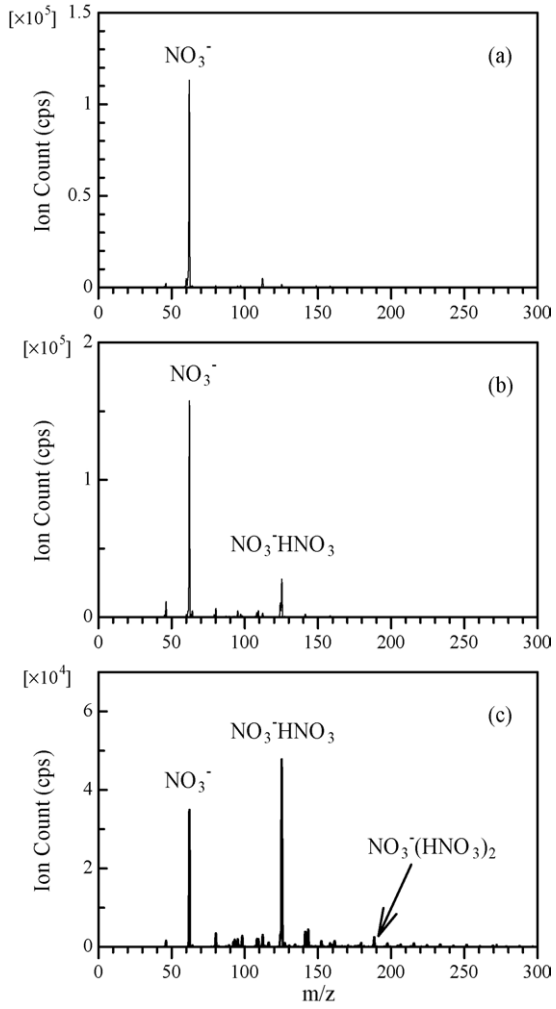

Fig. 3. Dependence of negative ion mass spectra in purified air on the concentration of H_2O: (a) $[H_2O] = 25$ ppm; (b) 1.1×10^3 ppm; (c) 6.1×10^3 ppm.

became larger. At a H_2O concentration of 6.1×10^3 ppm, the signal of $HNO_3{}^-HNO_3$ exceeded that of $NO_3{}^-$. In addition, $HNO_3{}^-(HNO_3)_2$ appeared, indicating that the concentration of HNO_3 had increased substantially. Consequently, it is clear that HNO_3 production increases with increasing H_2O concentration.

The formation of HNO_3 is thought to proceed by the reaction shown below [18]:

$$NO_2 + OH + M \rightarrow HNO_3 + M,$$
$$k_{10} = 3.3 \times 10^{-30}\,\mathrm{cm^6/s} \quad (10)$$

Since the concentration of NO_2 did not show any significant dependence on the concentration of H_2O, the production of OH radicals seems likely to be enhanced by the increase in H_2O concentration.

3.4. Formation of OH

More direct evidence of the formation of OH radicals can be found in the spectrum of ions produced in a shorter reaction time using purified air, as shown in Fig. 4. In the spectrum, $OH^-(H_2O)_n$ were clearly observed while $O_3{}^-(H_2O)_n$ and

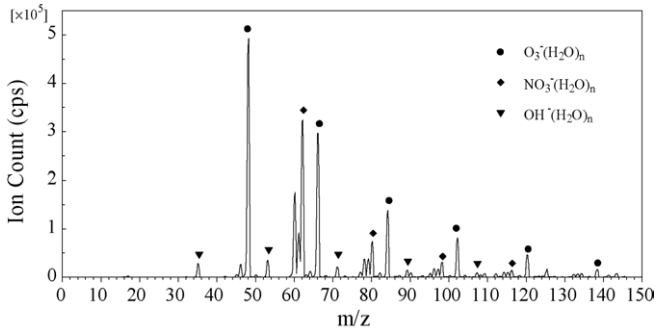

Fig. 4. Negative ion mass spectrum in purified air. The reaction time was 1.0 ms: $[H_2O] = 1.1 \times 10^3$ ppm.

$NO_3{}^-(H_2O)_n$ ions were predominant. The yield of $OH^-(H_2O)_n$ varied depending on the concentration of H_2O. Fig. 5 shows the relative abundance of $OH^-(H_2O)_n$ ions, which increased with the concentration of H_2O. This dependence implies that OH^- ions resulted from a reaction involving H_2O. The reaction of O^- and H_2O appears to be the most probable reaction for explaining the dependence [16]:

$$O^- + H_2O \rightarrow OH^- + OH, \qquad k_{11} = 6 \times 10^{-13}\,\mathrm{cm^3/s} \quad (11)$$

If this reaction is responsible for observed OH^- ions, OH must be simultaneously produced, which probably accounts for the formation of HNO_3 as discussed above. In air rich in O_3 and NO_2, OH^- can be further converted to neutral OH by the reaction with O_3 and NO_2 [15]:

$$OH^- + O_3 \rightarrow O_3^- + OH, \qquad k_{12} = 9 \times 10^{-10}\,\mathrm{cm^3/s} \quad (12)$$

$$OH^- + NO_2 \rightarrow NO_2^- + OH, \qquad k_{13} = 1.1 \times 10^{-9}\,\mathrm{cm^3/s} \quad (13)$$

3.5. Formation of $HCO_3{}^-$ ions

We initially assumed that the ion with $m/z = 124$ was due to $NO_3{}^-$ ions. Unlike $NO_3{}^-$ and $NO_3{}^-HNO_3$ ions, however, this ion peak was prominent only in mass spectra obtained in ambient air. In mass spectra in purified air, the abundance of this ion was

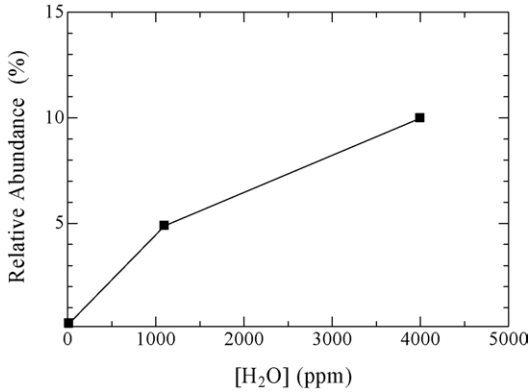

Fig. 5. Dependence of the relative abundance of $OH^-(H_2O)_n$ on the concentration of H_2O in purified air at a reaction time of 1.0 ms.

usually much smaller than that of $NO_3^-HNO_3$. To determine the neutral species responsible for this ion, we added NO_2, CO_2, and H_2O to the purified air. While the peak remained small in the presence of added NO_2 and H_2O, the addition of CO_2 and H_2O caused a substantial increase in the signal of this ion. This suggests that CO_2 is involved in the formation of the ion peak at $m/z = 124$. Since H_2O was also necessary for producing this ion, the contribution of OH and/or OH^- can be inferred. From these results, we presumed that OH^- reacts with CO_2 to form HCO_3^- [16]:

$$OH^- + CO_2 + M \rightarrow HCO_3^- + M,$$

$$k_{14} = 7.6 \times 10^{-28}\,cm^6/s \quad (14)$$

and the HCO_3^- ion is involved in the formation of the ion with $m/z = 124$. As a consequence, we assigned the $m/z = 124$ ion to $HCO_3^-HNO_3$.

The formation of HCO_3^- as one of terminal ions at 10^{-5} s under the tropospheric conditions was predicted by Huertas et al. by calculation [10]. In fact, the HCO_3^- ($m/z = 61$) ion was observed along with $HCO_3^-HNO_3$ in the spectrum in Fig. 2(a). It is interesting, however, that HCO_3^- almost disappeared and only a cluster ion of $HCO_3^-HNO_3$ remained when the reaction time was increased to about 10 ms, as shown in Fig. 2(b). In contrast, both HNO_3^- and $HNO_3^-HNO_3$ were present in the spectrum at comparable intensities, as shown in Fig. 2(b). This suggests that the association of HNO_3 with HCO_3^- was faster than that with NO_3^-.

3.6. Reactivity of NO_3^- and HCO_3^- ions in air

It has been shown that negative ions produced by a corona ionizer in air evolve into NO_3^-, $HCO_3^-HNO_3$, and $NO_3^-HNO_3$ within about 10 ms after ionization. The question arises as to how long these ions persist in air. Once NO_3^- ions are formed, they react only with molecules with greater electron affinities than that of NO_3. Since the electron affinity of NO_3 is greater than those of major air constituents, only a few compounds in air would be able to react with NO_3^- ions. One such molecule is H_2SO_4, and the reaction of NO_3^- with H_2SO_4 has been reported to proceed rapidly [19]:

$$NO_3^- + H_2SO_4 \rightarrow HSO_4^- + HNO_3,$$

$$k_{15} = 2.6 \times 10^{-9}\,cm^3/s \quad (15)$$

However, the concentration of H_2SO_4 in air is usually very small and it takes time for the conversion of NO_3^- ions into HSO_4^- ions. According to the calculation by Luts [11], HSO_4^- ions dominate over NO_3^- ions at about 80 s after ionization in unpolluted air. This time may be comparable to the lifetime of the ion in indoor air (<100 s).

There have been a few studies reported on the reactivity of HCO_3^-. The binary reaction of HCO_3^- with SO_2 to form HSO_3^- has been reported to be rapid [16]. Since the concentration of SO_2 is normally higher than that of H_2SO_4, the lifetime of HCO_3^- may be shorter than that of NO_3^-. However, the fate of HSO_3^- is not certain. Another reported reaction relevant to HCO_3^- ion is the one between $HCO_3^-(H_2O)$ and HCOOH to give HCO_3^-HCOOH [20], but it is of little importance except for an environment in which the concentration of HCOOH is extremely high. No other reactions have been reported.

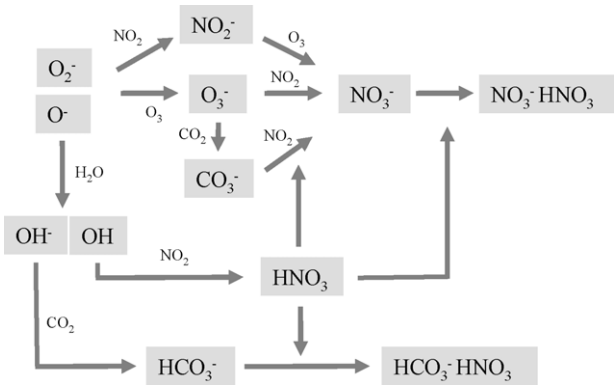

Fig. 6. Reaction scheme for the evolution of negative ions in air by a corona ionizer.

4. Summary

Although the evolution time observed in this study was only a small fraction of the total ion lifetime, several features of the evolution of negative ions produced by a corona ionizer were revealed.

First, O_3 and NO_2 generated by discharge were shown to strongly influence the early stages of the negative ion evolution. These byproducts efficiently lead to the dominance of NO_3^- ions.

More importantly, the presence of H_2O was found to be a crucial factor in controlling the terminal ion species and their lifetimes. H_2O is the source of OH, and can lead to the formation of a large amount of HNO_3. This accelerates the conversion of primary negative ions to NO_3^- ions, forming NO_3^- and $NO_3^-HNO_3$ terminal ions. H_2O also serves as a source of OH^- which reacts with CO_2 to form HCO_3^-. The $HCO_3^-HNO_3$ cluster ion was one of the terminal ions observed in this study. The reaction scheme for explaining this series of reactions is described in Fig. 6. It should be noted, however, that the scheme may be modified under different operating conditions of corona discharges or when different types of discharges are employed because the rates of production of O_3, NO_2, as well as O^- (which can produce OH and OH^- by reaction with H_2O) could be affected by such changes. Considering ion reactivity, NO_3^- ions are likely the most long-lived ion species in negative ion evolution in indoor air.

Corona discharge ionizers have been actively utilized in the techniques of atmospheric pressure chemical ionization mass spectrometry (APCIMS) and ion mobility spectrometry (IMS) as non-radioactive ionization sources [7,8,21]. The results of the present study also provide additional information on the process by which both reactant ions and product ions are formed in these techniques.

Acknowledgement

This work was partly sponsored by Grant-in-Aid for Scientific Research (B) from Ministry of Education, Culture, Sports, Science and Technology of Japan (11558066, 12018209, 13878098).

References

[1] S.L. Daniels, IEEE Trans. Plasma. Sci. 30 (2002) 1471.
[2] C.C. Wu, G.W.M. Lee, Atmos. Environ. 38 (2004) 6287.
[3] M.M. Shahin, Appl. Opt., Suppl. Electrophotography 3 (1969) 106.
[4] P.S. Gardiner, J.D. Cragss, J. Phys. D: Appl. Phys. 10 (1977) 1003.
[5] B. Gravendeel, F.J. de Hoog, J. Phys. B: Mol. Phys. 20 (1987) 6337.
[6] S. Sakata, T. Okada, J. Aerosol Sci. 25 (1994) 879.
[7] S.K. Ross, A.J. Bell, Int. J. Mass Spectrom. 218 (2002) L1.
[8] C.A. Hill, C.L.P. Thomas, Analyst 128 (2003) 55.
[9] J.D. Skanly, T. Mikoviny, S. Matejcik, N.J. Mason, Int. J. Mass Spectrom. 233 (2004) 317.
[10] M.L. Huertas, J. Fontan, J. Gonzalez, Atmos. Environ. 12 (1978) 2351.
[11] A. Luts, J. Geophys. Res. 100 (1995) 1487.
[12] K. Nagato, C.S. Kim, M. Adachi, K. Okuyama, J. Aerosol Sci. 36 (2005) 1036.
[13] J. Skalny, R.S. Sigmond, Book of Contributed Papers of the 16th ICPIG, Düsseldolf (1983) 554.
[14] P. Watts, Int. J. Mass Spectrom. Ion Proc. 121 (1992) 141.
[15] Y. Ikezoe, S. Matsuoka, M. Takebe, A.A. Viggiano, Gas Phase Ion–Molecule Reaction Rate Constants Through 1986, Maruzen, Tokyo, 1987.
[16] F.C. Fehsenfeld, E.E. Ferguson, J. Chem. Phys. 61 (1974) 3181.
[17] O. Möhler, F. Arnold, J. Atmos. Chem. 13 (1991) 33.
[18] R. Atkinson, D.L. Baulch, R.A. Cox, J.N. Crowley, R.F. Hampson, R.G. Hynes, M.E. Jenkin, M.J. Rossi, J. Troe, Atmos. Chem. Phys. 4 (2004) 1461.
[19] A.A. Viggiano, R.A. Perry, D.L. Albritton, E.E. Ferguson, F.C. Fehsenfeld, J. Geophys. Res. 87 (1982) 7340.
[20] J. Viidanoja, T. Reiner, F. Arnold, Int. J. Mass Spectrom. 181 (1998) 31.
[21] E. Nikolaev, L.S. Reiter, B.C. Laughlin, E. Handberg, R.G. Cook, Eur. J. Mass Spectrom. 10 (2004) 197.